Bull. Soc. géol. France, 2013, t. 184, n° 4, pp. 377-387

Relations between the scaling exponents, entropies, and energies of fracture networks

AGUST GUDMUNDSSON[1*] and NAHID MOHAJERI[2]

Keywords. – Tension fractures, Earthquake faults, Power laws, Crustal stresses, Plate boundaries, Thermodynamics, Iceland.

Abstract. – Fracture networks commonly show power-law length distributions. Thermodynamic principles form the basis for understanding fracture initiation and growth, but have not been easily related to the power-law size distributions. Here we present the power-law scaling exponents and the calculated entropies of fracture networks from the Holocene part of the plate boundary in Iceland. The total number of tension fractures and normal faults used in these calculations is 565 and they range in length by five orders of magnitude. Each network can be divided into populations based on 'breaks' (abrupt changes) in the scaling exponents. The breaks, we suggest, are related to the comparatively long and deep fractures changing from tension fractures into normal faults and penetrating the contacts between the Holocene lava flows and the underlying and mechanically different Quaternary rocks. The results show a strong linear correlation (r = 0.84) between the population scaling exponents and entropies. The correlation is partly explained by the entropy (and the scaling exponent) varying positively with the arithmetic average and the length range (the difference between the longest and the shortest fracture) of the populations in each network. We show that similar scaling laws apply to other lineaments, such as streets. We propose that the power-law size distributions of fractures are a consequence of energy requirements for fracture growth.

Les relations entre exposants d'échelle, entropies et énergies des réseaux de fractures

Mots-clés. – Fractures de tension, Failles sismiques, Lois puissance, Contraintes crustales, Frontière de plaque, Thermodynamique, Islande

Résumé. – La distribution des longueurs de réseaux de fractures suit souvent une loi de puissance. Les principes thermodynamiques constituent une base pour comprendre l'initiation et la croissance des fractures, mais ne sont pas facilement reliés à des distributions en loi de puissance. Nous présentons ici les exposants d'échelle en loi de puissance et les entropies calculées de réseaux de fractures holocènes de la frontière de plaque divergente en Islande. Le nombre total de fractures de tension et de failles normales utilisées dans ces calculs est de 565 et l'ordre de grandeur de leurs longueurs va de 1 à 5. Chaque réseau peut être divisé en populations sur la base de changements brusques (« breaks ») dans les exposants d'échelle. Ces changements brusques sont liés à des fractures relativement longues et profondes, évoluant de fractures de tension en failles normales et traversant les coulées de lave holocènes et les roches quaternaires sous-jacentes, mécaniquement différentes. Les résultats montrent une forte corrélation linéaire (r = 0,84) entre les exposants d'échelle de la population et les entropies. Cette corrélation s'explique en partie par l'entropie (et l'exposant d'échelle) variant positivement avec la moyenne arithmétique et la fourchette des longueurs (la différence entre la plus longue et la plus courte fracture) des populations dans chaque réseau. Nous montrons que des lois d'échelle similaires s'appliquent à d'autres linéaments, comme les rues. Nous proposons que les distributions de taille de fractures suivant une loi de puissance soient une conséquence des besoins en énergie pour la croissance des fractures.

INTRODUCTION

Rock-fracture networks control many of the Earth's natural hazards such as volcanic eruptions and earthquakes, as well as the permeability of fractured reservoirs. How such networks form and develop is of fundamental importance in theoretical fields such as volcanotectonics and seismotectonics, and in more applied fields such as hydrogeology, petroleum geology, and engineering geology. There has been great progress in understanding fracture initiation and propagation in the past decades [e.g., Wei, 2010; Gudmundsson, 2011], but the overall development of complex fracture networks is still poorly understood and a matter of intensive research.

In rock-fracture networks or systems, the fracture-length size distributions commonly follow power laws in the form [Xie, 1993; Turcotte, 1997; Barabasi and Albert, 1999; Newman, 2005]:

$$P(\geq x) = Cx^{\gamma} \qquad (1)$$

where P(x) is the number or frequency of fractures with a length larger than x, C is a constant of proportionality, and γ is the scaling exponent. When the data are plotted using bins of given width or class limits, then all fractures in a

1. Department of Earth Sciences, University of London Royal Holloway, Egham TW20 0EX, UK. *Fax*: +44-1784-471-780.
E-mail address: a.gudmundsson@es.rhul.ac.uk. * corresponding author
2. Department of Geography, University College London, Gower Street, Pearson Building, London, WC1E 6BT, UK
Manuscript received on March 4, 2012; accepted on June 16, 2012

given bin exceed the length x. For example, if the bin width (class limits) of 100 m is used, then all fractures longer than 0 m fall into the first bin, all fractures longer than 100 m fall into the second bin, all fractures longer than 200 m fall into the third bin, and so on. On a bi-logarithm (log-log) plot, a power law such as Eq. (1) yields a straight line the slope of which is γ. Because the number of objects (here fractures) normally increases as they become smaller (shorter), the slope is negative. The scaling exponent, however, is defined as the negative of the slope, and is thus a positive number.

There has been much work on power-law size distributions of rock fractures in the past decades [e.g., Xie, 1993; Hatton *et al*., 1994; Turcotte, 1997; Bour and Davy, 1998; Berkowitz *et al*., 2000; Bonnet *et al*., 2001; Nieto-Samaniego *et al*., 2005]. While many ideas have been proposed as to the development of such power laws, as yet no clear and generally accepted links have been established between the statistical size distributions and the thermodynamic principles on which fracture mechanics rests [Griffith, 1920; Rice, 1978; Atkins and Mai, 1985; Stevens and Guiu, 1991; Wei, 2010].

In this paper we explore the connection between the scaling exponents and entropies of rock fractures using data from the networks of Reykjanes and Thingvellir, in southwest Iceland, and Krafla and Husavik in North Iceland (fig. 1). All the fractures are hosted by 9-10 ka old pahoehoe lava flows, with essentially uniform mechanical properties, and develop from roughly hexagonal cooling (columnar) joints and contacts between flow units [Gudmundsson, 1992, 2011].

The first aim of this paper is to present data on rock-fracture networks in Iceland with a view of understanding better their mechanical evolution. The focus is on the length-size distributions and scaling (power-law) exponents. The second aim is to present the entropies of the fracture populations and compare these with the associated scaling exponents, length ranges, and average lengths. The third aim is to explore the linear correlation between the scaling exponents and the entropies of the fracture populations in terms of general mechanical considerations, including energy input for lineament development, with a brief comparison between fractures and streets.

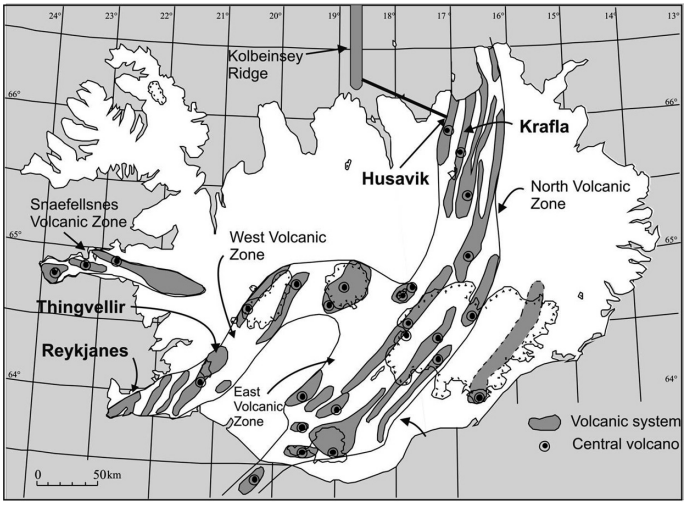

FIG. 1. – Location of the fracture networks within the active volcanic systems of the plate boundary in Iceland. The fracture networks are referred to as Reykjanes, Thingvellir, located in the West Volcanic zone, and Husavik and Krafla, located in the North Volcanic zone. More specifically, the fractures in the Husavik network are located at the junction between the North Volcanic zone, a rift zone, and the Husavik-Flatey fault, a transform fault that connects the North Volcanic zone with the Kolbeinsey ridge.

FRACTURE NETWORKS

The fractures were studied in four main networks located within the active volcanic rift zone (the divergent plate boundary) of Iceland (fig. 1). All the fractures occur in Holocene pahoehoe lava flows (figs. 2-3). The lava flows form parts of lava shields formed in the early postglacial period, mostly 9-10 ka old [Rossi, 1996; Andrew and Gudmundsson, 2007; Thordarson and Hoskuldsson, 2008]. The pahoehoe lava flows formed over many years, some over tens of years. Some reach thicknesses of as much as several hundred metres and volumes great as 20 km^3.

FIG. 2. – Tension fracture in Thingvellir, Southwest Iceland (fig. 1). View northeast, the fracture is partly filled with groundwater and the size of its opening (aperture) is mostly 10-15 m. In the fracture walls there are columnar joints, from which all the large-scale fractures develop [cf. Gudmundsson, 1987b].

FIG. 3. – Part of the western boundary (normal) fault, Almannagja, at Thingvellir, Southwest Iceland. Aerial view southwest, this boundary fault is mixed-mode: partly a tension (mode I) fracture, and partly a shear (here mode III) fracture. The maximum opening (aperture) seen here is about 40 m. When referring to the lowest ground on the eastern (left-hand) side of the fault, the maximum displacement is about 35 m [cf. Gudmundsson, 1987b].

All the fractures originate from hexagonal columnar (cooling) joints in the lava flows. During rifting episodes the joints link up into larger offset fracture segments that gradually propagate and link into still larger fractures (figs. 2-3). The pahoehoe lava flows have essentially uniform mechanical properties, the in-situ estimates of the static Young's modulus being in the range of 3-5 GPa and those of Poisson's ratio at about 0.25 [Gudmundsson, 2011].

The fractures are of two main types: tension fractures (fig. 2) and normal faults (fig. 3). The tension fractures form during rifting events when there is absolute tension in the uppermost part of the crust, that is, the minimum principal compressive stress, σ_3, is negative. Tension fractures thus differ from the other main type of extension fractures, namely fluid-driven fractures (hydrofractures), in that for a tension fracture to form the regional σ_3 must be negative, whereas for most extension fractures (dykes, sills, and man-made hydraulic fractures, as well as many joints and mineral veins) σ_3 is positive (compressive; cf. Gudmundsson [2011]). At the time of tension-fracture formation, the tensile stress must be equal to the tensile strength of the pahoehoe lava flow hosting the tension fracture, that is, some 1-6 MPa. Some of the tension fractures are large, with apertures or openings of more than ten metres and lengths or strike dimensions of several hundred metres (fig. 2). It follows from the Griffith criterion that tension fractures cannot exceed depths of about 1 km; to reach greater depths they must change into normal faults [Gudmundsson, 1992; Jaeger *et al*., 2007].

Most of the tension fractures in the study areas (fig. 2) presumably have depths (dip dimensions) from several metres to hundreds of metres. Tension fractures that develop within an essentially homogeneous, isotropic rock body, such as a pahoehoe lava flow, and are subject to uniform tensile stress, tend to become circular or penny-shaped, whereas those extending from the surface and into the body tend to become semi-circular [Atkins and Mai, 1985; Gudmundsson, 2011]. Comparatively few tension fractures reach many hundred metres in length, and most are less than one hundred metres. It follows that the tension-fracture depths are mostly in the range of metres to a few hundred metres. The latter figure is also the common thicknesses of the Holocene pahoehoe lava flows [Rossi, 1996; Andrew and Gudmundsson, 2007; Thordarson and Hoskuldsson, 2008], implying that most of the tension fractures are located within the lava flows themselves and do not penetrate into the underlying Pleistocene rocks.

The normal faults (fig. 3) are generally much longer than the tension fractures. For example, of 120 tension fractures and normal faults studied in the network or swarm on Reykjanes, the average length of the tension fractures is 370 m whereas that of the normal faults is 1990 m [Gudmundsson, 1987a] – bearing in mind that 'average' length is a poor measure of the most typical length of a power-law size distribution. This suggests that many of the tension fractures change into normal faults when they reach the critical depths of several hundred metres [Gudmundsson, 1992; Jaeger *et al*., 2007].

POWER LAWS

The fracture lengths range from about 0.1 m to close to 8 km, that is, by close to five orders of magnitude (figs. 4, 5; table I). The shortest fractures are tension fractures (fig. 2) formed through reopening of columnar joints, whereas the longest ones are normal faults formed through the linkage of many shorter segments (fig. 3).

The bi-logarithmic (log-log) plots of the fracture lengths (figs. 4, 5) show that the single straight-line relationships hold only over restricted lengths. Thus, each data set is better approximated by two straight lines (Similar breaks have also been observed in the relation between length and maximum opening of tension fractures in Iceland [Hatton *et al*., 1994]). The breaks in the straight-line slopes occur at the following fracture lengths (table I): for Reykjanes at 500 m, for Thingvellir at 300 m, for Reykjanes and Thingvellir combined at 300, and for the whole data set, including the short fractures at Krafla and Husavik in North Iceland (fig. 1) at 500 m.

The breaks can be related to two factors that encourage a change in the fracture development, namely (i) the change of tension fractures into normal faults and (ii) the change in the host-rock properties at depth. From the Griffith criterion for rocks [Griffith, 1920; Jaeger *et al*., 2007], it follows that the tension fractures must change into normal faults on reaching a certain depth [Gudmundsson, 1992; Jaeger *et al*., 2007]. For semi-circular fractures, this depth is equal to half the surface length (strike dimension), or 150-250 m (for lengths of 300-500 m). For a typical Holocene lava flow (host-rock) tensile strength of 1-2 MPa and a density of 2500 kg m^{-3} [Gudmundsson, 2011], the depth at which this change occurs would be 120-240 m.

This depth is also similar to the estimated thicknesses of the Holocene lava flows in Thingvellir and Reykjanes [Rossi, 1996; Andrew and Gudmundsson, 2007; Thordarson and Hoskuldsson, 2008]. At the bottom of the Holocene flows, abrupt changes in stiffness, and weak or open contacts, are likely to occur, resulting in a change in the style of fracturing. For example, the fractures confined to the Holocene flows may act as through-cracks (partly due to numerous weak and open contacts between the flow units), whereas those that penetrate into the deeper layers, primarily as normal faults, may act as part-through cracks [Atkins and Mai, 1985; Gudmundsson, 2011].

On inspection the fracture data seem to fit power-laws quite well (figs. 4-5). There exist, however, several tests that can be used to check the goodness-of-fit between the calculated power-law curves and the actual data. One test uses the residuals of the curve-fitting procedure, that is, the vertical distances of all the points from the regression line [Mohajeri and Gudmundsson, 2012]. Another test uses the maximum likelihood method to compare the power-law fits with log-normal, exponential, and stretched exponential fits. Using such tests, we found that for some fracture populations, such as those discussed above, power-law models fit the data very well, whereas for a few populations other models such as log-normal or stretched exponential models might be provide better fits than power laws [Mohajeri and Gudmundsson, 2012].

The main reason that we use the power-law models, however, has less to do with the exactness of the power-law fit rather than with the opportunity that such models offer to

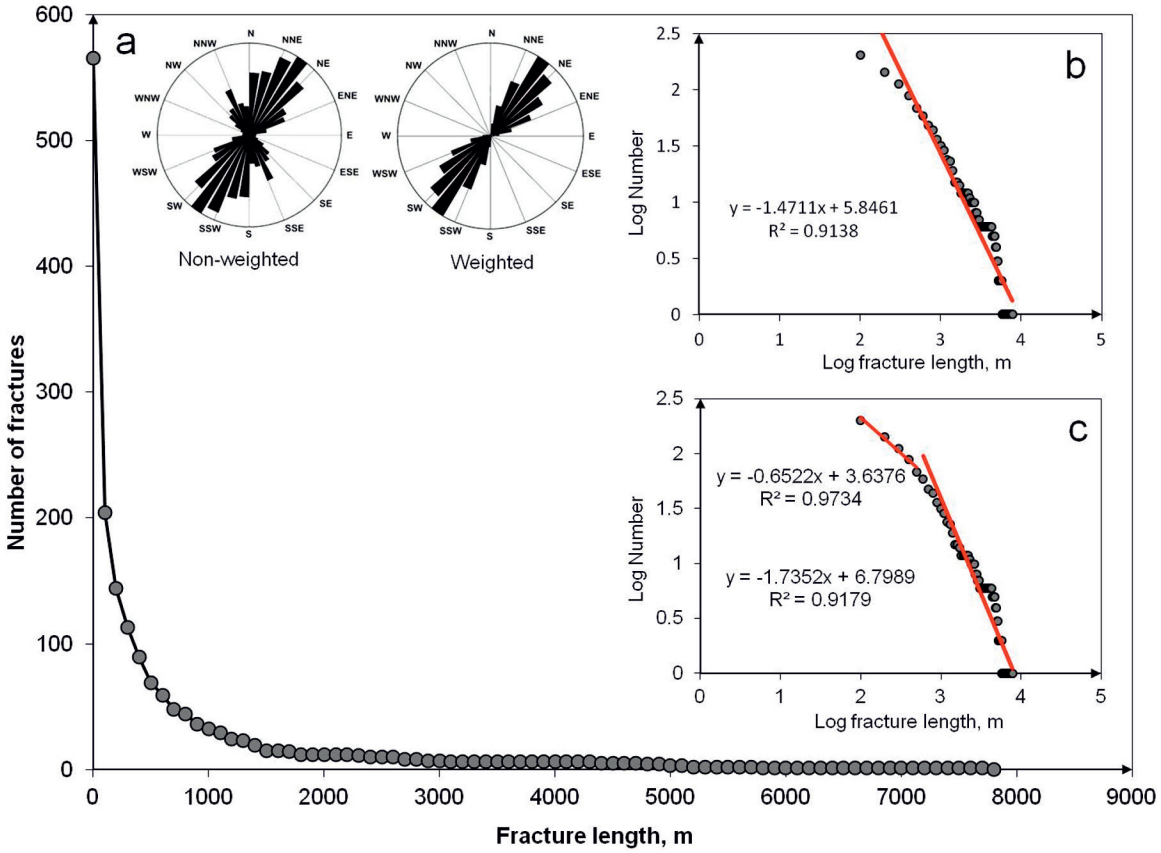

FIG. 4. – Power laws and breaks in scaling exponents for all the analysed fractures, a total of 565 fractures in four networks. (a) A cumulative power-law distribution for fracture lengths, and rose diagrams for fracture strike (inset), non-weighted to the left and weighted to the right. The fractures are normalised or weighted by selecting the shortest fracture as a unit and dividing each fracture by that unit. This means that long fractures count as many fractures in the weighted rose diagram. The length range is 0.1-6636 m and the average length is 249 m. (b) Bi-logarithmic (log-log) plot of all the fractures using a single power law. (c) Bi-logarithmic plot of all the fractures using two (double) power laws. The break in the straight-line slopes indicates different fracture (sub)populations. The estimated coefficients of determination (R^2) of the two associated fracture subpopulations are indicated.

use different scaling exponents, determined from log-log plots, to divide fractures into different populations. As we suggest below, the populations determined in this way yield different length ranges and entropies which offer information on their mechanics of formation.

ENTROPY

In statistical mechanics and information theory, entropy has a probability basis through the number of microstates available to a certain macrostate of a system. The entropy S for a general probability distribution (here the length-frequency distribution of fractures) is [Baierlein, 1971, 1999; Laurendeau, 2005; Volkenstein, 2009]:

$$S = -k\sum_{i=1}^{t} p_i \ln p_i \qquad (2)$$

where k is a constant, the meaning of which is discussed below. For the cumulative power-law size distributions in figures 4 and 5, t is the number of classes or bins that contain fractures in the frequency distribution, that is, the number of bins with nonzero probabilities of fractures. Similarly, p_i is the probability of fractures belonging to the i-th bin, that is, the probability of the i-th class or bin. Thus, for example, if the number (or the cumulative number as in the present analysis) of the fractures in a population is 600 and the number of fractures falling into the sixth bin is 30, then p_i for the sixth bin is 30/600 = 0.05. The negative sign of k in Eq. (2) is because probability is always between 0 and 1, and the natural logarithm of numbers between 0 and 1 is negative. Thus, to get a positive value for the entropy, as it must be, there is a minus sign. Equation (2) presents a perfectly general relation between entropy S and probability p_i and is equally valid for equilibrium and non-equilibrium systems.

When calculating the entropy using Eq. (2) only those bins that contain at least one observed fracture are included. By definition:

$$\sum_{i=1}^{t} p_i = 1 \qquad (3)$$

so that the sum of the probabilities for all the bins equals one. The probabilities as applied to fractures in a network or population are a measure of the chances of a randomly selected fracture from the population falling into a particular bin.

There are two topics that need further discussion before applying Eq. (2) to fracture-length size distributions. One is the effect of the widths or the sizes of the classes or bins used in grouping the data in the distribution. The other is the meaning of the constant k. Both points relate to aspects of statistical mechanics and thermodynamics, on one hand,

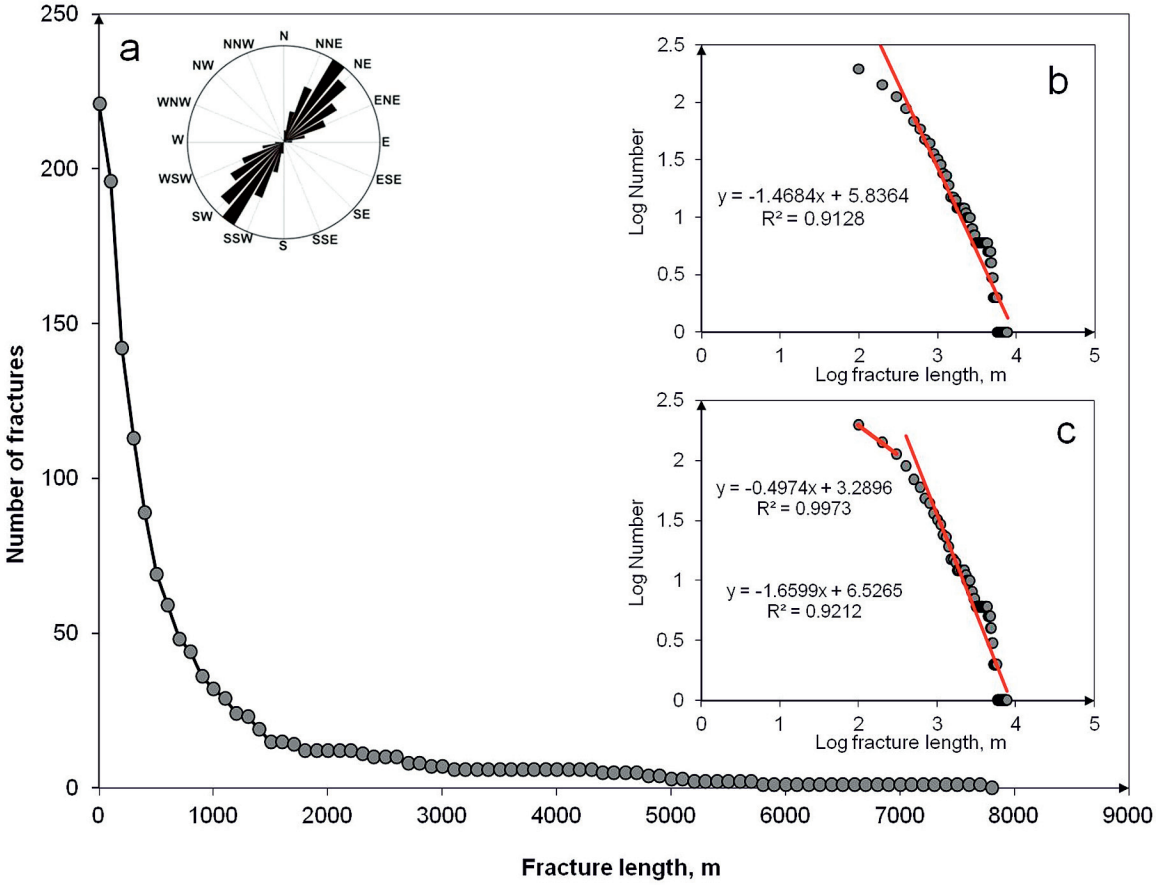

FIG. 5. – Power laws and breaks in scaling exponents for the analysed combined fracture networks in Southwest Iceland. (a) A cumulative power-law distribution for fracture lengths, and a rose diagram for fracture strike (inset), for the combined Reykjanes-Thingvellir network. Total number of fractures, N, is 221 and their lengths range from 40 m to 7736 m. (b) A bi-logarithmic (log-log) plot of the Reykjanes-Thingvellir fractures showing the break in the straight-line slopes. The estimated coefficients of determination (R^2) of the two associated fracture subpopulations are indicated.

and information theory, on the other. A detailed discussion is beyond the scope of the present paper but a brief summary of the main points is appropriate.

We tested the effects of bin size on entropy for the combined fracture population from Husavik and Krafla, a total of 344 small tectonic fractures (fig. 1). We used this combined population rather than that of Reykjanes-Thingvellir (fig. 1) because small bin widths (such as 1-20 m) are not possible for the large fractures. This follows because the number of bins cannot exceed the number of fractures or other objects that are being binned. The results (fig. 6) show that the calculated entropy decreases as the bin width increases, in agreement with other studies [e.g., Singh, 1997; Mays *et al.*, 2002]. To take the bin width into account, the term , where b is the bin width, should be added to Eq. (2). Here, however, all the bin widths used are equal, that is, 100 m, allowing a direct comparison between the calculated entropies of the fracture populations (table I).

For thermodynamic entropy, k in Eq. (2) is Boltzmann's constant (k_B) and has the value of $k_B = 1.38065\ 10^{-23}$ J K^{-1}. For general probability or frequency distributions (fig. 1), k is commonly regarded as an arbitrary constant with a unit value, in which case the entropy calculated through Eq. (2) is dimensionless. In fact, if temperature is defined in units of energy, as it common in physics, rather than in terms of the Kelvin temperature scale, as above, then the thermodynamic entropy would be dimensionless [e.g., Leff, 1999; Sethna, 2006; Ben-Naim, 2008] and, therefore, more easily interpreted as a measure of 'missing information' or 'degree of uncertainty' as regards a system [Sethna, 2006; Blundell and Blundell, 2010]. Boltzmann's constant may be

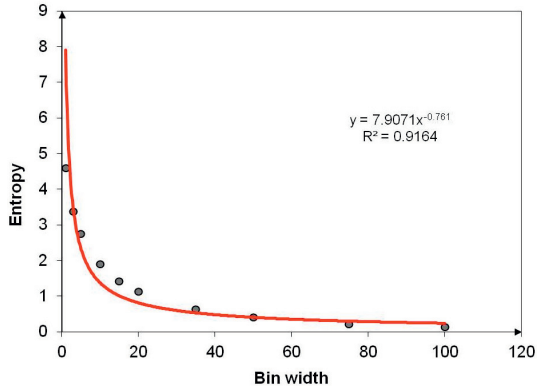

FIG. 6. – Inverse relationship between entropy and bin (class) width or size for the fracture networks in North Iceland (fig. 1). As the bin width gradually increases from 1 m to 100 m, the corresponding entropy decreases from 4.588 to 0.143. For comparing entropies of lineament populations, the bin width should be constant - as it is in all the analyses in this paper, namely 100 m (table I).

regarded as a conversion factor between the units of energy and the units of temperature and related to the fact that we commonly measure temperature and energy using different scales [Sethna, 2006]. Thus, multiplying the entropies in table I by the value of k_B would give us the units of thermodynamic entropy. Missing information (MI) is another name for 'information entropy', a concept widely regarded as providing one of the foundations of statistical mechanics [Jaynes 1957a,b; Baierlein, 1971; Laurendeau, 2005; Ben-Naim, 2008; Volkenstein, 2009]. In particular, there is a general correspondence between information and thermodynamic entropies for systems in equilibrium [Baierlein, 1971]. The fracture populations in the present study (fig. 1) may be regarded as systems in equilibrium except during volcanotectonic episodes. Recent experimental demonstration for converting information into energy [Toyabe *et al.,* 2010] is a further support for the connection between information and statistical mechanics.

The entropies calculated in this paper (table I) are dimensionless, and are thus given in units of *nat*. This is equivalent to Boltzmann's constant k_B being normalised to a factor 1. If the logarithmic base used were 2 rather than e (as here for the natural logarithm), then the normalisation of k_B would result in entropies given in the units of *bits* [e.g., Sethna, 2006]. Although the entropies in table I are dimensionless, their physical connection to development of the fracture networks becomes clear in later sections. This follows because, as is discussed below, fracture formation and propagation requires energy. From the theory of fracture mechanics it follows that the longer the fracture, other things being equal, the greater must be the energy input to develop the fracture up to that length. The fracture development also produces entropy which is reflected in the entropy calculated from the power-law size distributions of the fracture populations (figs. 4,5).

CORRELATION BETWEEN ENTROPY AND SCALING EXPONENT

We divide the fractures into four main populations: Reykjanes, Thingvellir, Reykjanes-Thingvellir combined, and Reykjanes, Thingvellir, Krafla, and Husavik combined (fig. 1, table I). The reason that we do not include the Krafla and Husavik data sets as separate populations is that their fractures are very short, ranging in length from 0.1 m to 270 m, with the great majority of the fracture being less than 10 m long. It follows that a bin width of 100 m, as used for all the fracture populations here, is not suitable for the data sets at Krafla and Husavik, although these sets fit very well in as parts of the combined total set – with a length range of 0.1 m to 7736 m.

Each of the four main populations can be divided further into two subpopulations based on the break in the straight-line slopes on the bi-logarithmic plots (figs. 4, 5). We have calculated the entropy and scaling exponent for 12 populations (table I). The results show a strong correlation between the entropy and the scaling exponent of the fracture populations (fig. 7a). The coefficient of determination for the 12 populations is $R^2 = 0.8428$ and the linear correlation coefficient is $r = 0.9180$. Since R^2 measures the ratio between the explained variation to the total variation, it follows that about 84% of the variation in entropy can be explained in terms of variation in scaling exponent.

A long power-law tail normally implies a dispersed statistical distribution and a comparatively high entropy. Not only that, but as the tail becomes longer and flatter, the distribution becomes more similar to a uniform distribution – and a uniform distribution has generally the highest entropy. The entropy might therefore be expected to vary positively with the length of the tail. Thus, the entropy should increase with increasing range in length (the difference between the maximum and the minimum length) as well as with increasing average length of fractures within the subpopulations of each network. To test this possibility, we plotted the entropies of the fracture populations against their length ranges and average lengths. The results show high linear correlations between the entropy and the length range as well as between the entropy and the average length (figs. 7b, 7c). The results suggest that the calculated entropies (and scaling exponents) of the fracture populations may be regarded as a measure of the dispersion of fracture lengths in the populations as they develop and expand over time.

DISCUSSSION

The changes in scaling exponent and entropy of fracture networks can be broadly understood as follows. As the loading on a rock laboratory specimen or a volcanic system (figs. 1) increases fractures start to develop. In the laboratory specimen, the fractures develop from pores (cavities) and crystals [Xie, 1993], whereas in a volcanic system they commonly develop from previously formed (existing) larger weaknesses such as columnar joints (fig. 3) [Gudmundsson, 1992]. The development of fracture networks similar to those observed in the laboratory and in the field (figs. 2-3) is not limited to rocks: most heterogeneous materials when subject to sufficiently high loading develop similar fracture networks [e.g., Mishnaevsky, 1998, 2007].

Many rock-physics experiments on the development of fracture networks are summarised by Xie [1993]. Commonly, the network nucleates at a notch, an area of stress

TABLE I. – Data on the 12 fracture populations (and subpopulations) analysed in the paper. The four main populations/networks are Reykjanes, Thingvellir, Reykjanes-Thingvellir and all the fracture data combined The number of fractures is listed in the second column, their mean strike in the third column, the standard deviation in strike in the fourth column, the length range in the fifth column, and the arithmetic average length in the sixth column. The scaling exponents (γ) and the entropies (*S*) of the 12 populations are presented in the seventh and eight columns. Many of the results are plotted in figure 7.

Table 1: Fracture data

Population	Number	Mean strike	Std. dev. of strike	Length range (m)	Average Length	$P(\geq x) = Cx^{-\gamma}$	$S = -\sum_{i=1}^{t} p_i \ln p_i$
				40-5750	614	γ=1.410	3.098
Reykjanes	120	55.38	17.86	40-500	232	γ= 0.612	1.716
				500-5750	1409	γ= 1.720	3.380
				57-7736	620	γ= 1.173	3.369
Thingvellir	101	29.31	11.10	57-300	169	γ= 0.554	1.347
				300-7736	1138	γ= 1.257	3.766
				40-7736	617	γ= 1.460	3.246
Reykjanes-Thingvellir	221	43.47	19.95	40-300	158	γ= 0.497	1.353
				300-7736	1055	γ= 1.659	3.578
				0.1-7736	249	γ= 1.471	2.902
All data	565	119.97	135.28	0.1-500	79	γ= 0.652	1.497
				500-7736	1472	γ= 1.735	3.676

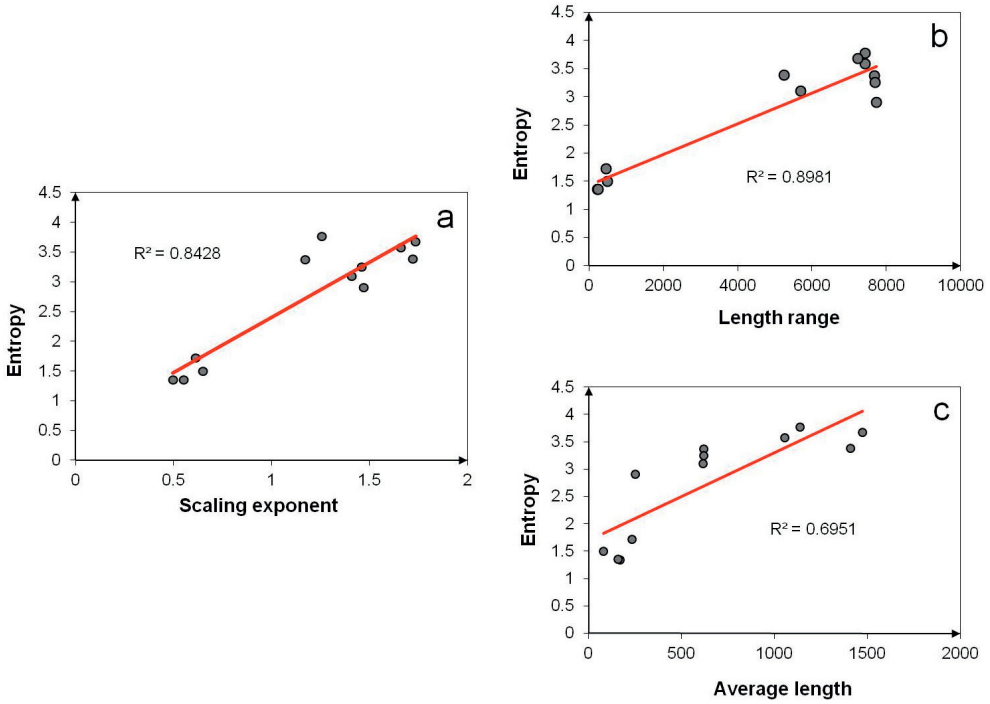

FIG. 7. – Linear correlation between the entropies, scaling exponents, length ranges, and average lengths of the 12 fracture (sub)populations in table I, with the corresponding coefficients of determination (R^2). (a) Correlation between entropy and scaling exponent. (b) Correlation between entropy and length range of fractures. (c) Correlation between entropy and average length of fractures.

concentration [Jaeger *et al.*, 2007; Gudmundsson, 2011], from which the fractures propagate and spread in various directions as the load is increased. The fractures link up to form gradually longer fractures as the fractured or damaged area expands, until the specimen fails when it forms a through-going fracture [Xie, 1993].

Rock-physics results show that as the fracture network expands, that is the material damage increases, more fractures initiate, propagate, and link together and the scaling exponent of the fracture population increases. For example, experiments on marble, a stiff (high Young's modulus) rock, show that as the fracture network expands, there is an increase in scaling exponent from about 1.7 to about 2.5 [Xie, 1993]. Similar results are obtained for softer (more compliant) rocks. For example, as a fracture network in a sandstone specimen expands during loading to failure, the scaling exponent increases from about 2.7 to about 2.9 [Xie, 1993]. Experiments also confirm that as the material damage increases, so does the entropy [Bao *et al.*, 2010; Naderi *et al.*, 2010]. Similarly, for the fracture networks in Iceland, there is a strong linear correlation between the entropy and the scaling exponents (fig. 6).

Griffith's theory

The power-law size distribution of the fracture populations (figs. 4, 5) can be explained in terms of Griffith's theory of fracture which derives from thermodynamic considerations of the global balance of energy in a solid body with existing flaws or micro-cracks [Griffith, 1920; Rice, 1978; Atkins and Mai, 1985; Stevens and Guiu, 1991; Wei, 2010]. The theory considers (1) the energy stored as potential (including strain) energy in the solid, (2) the energy needed to generate a new crack surface, and (3) the work performed during the crack growth by the loads on the body.

The total energy U_t of the thermodynamic system is given by:

$$U_t = \Pi + W_s \tag{4}$$

where Π is here the potential energy of the that part of the plate boundary segment which hosts the fracture network, and W_s is the surface energy or work needed to generate two new fracture surfaces. There are two possible sources of the potential energy: (1) the internal strain energy U_o stored in the plate boundary segment prior to fracture propagation, and (2) the work W_L done on the boundary through the generalised plate-tectonic forces F operating on the boundary while the fracture propagates.

For a fracture to propagate, the total energy U_t (Eq. 4) must be large enough to overcome the surface energy W_s. If the fracture is to propagate, U_t must either remain constant or decrease. For fracture growth under equilibrium conditions, whereby U_t = constant, we can differentiate Eq. (4) with respect to the new fracture surface area dA to obtain:

$$\frac{dU_t}{dA} = \frac{d\Pi}{dA} + \frac{dW_s}{dA} = 0 \tag{5}$$

It follows that:

$$-\frac{d\Pi}{dA} = \frac{dW_s}{dA} \tag{6}$$

Using Eq. (6) we may define the energy release rate G as:

$$G = -\frac{d\Pi}{dA} \tag{7}$$

which is the energy available to drive the fracture propagation. More specifically, fracture propagation occurs if the energy release rate G reaches the value:

$$G_c = \frac{dW_s}{dA} \quad (8)$$

which is the right-hand side of Eq. (6). This critical energy release rate for fracture to propagate, G_c, is known as the material toughness of the rock.

The surface energy W_s must be overcome, and thus put into the plate boundary segment for the fracture to propagate. Equations (5-8) refer to fracture surface A, but can also be rewritten in terms of fracture length (half-length for a central fracture) a. For example, the plane-strain energy release rate of a tension (mode I) fracture in terms of applied tensile stress σ is given by [e.g., Anderson, 2005; Gudmundsson, 2011]:

$$G_I = \frac{\sigma^2(1-\nu^2)\pi a}{E} \quad (9)$$

where E is Young's modulus and ν is Poisson's ratio of the host rock. For a normal fault modelled as mode II crack (as would be appropriate for a 'part-through crack' model of a normal fault – see Gudmundsson [2011], the driving shear stress $_d$ is substituted for σ in Eq. (9). A normal fault that extends from the surface of the rift zone to a magma reservoir, such may apply to some of the large normal faults studied here (fig. 3), a mode III through-crack model is appropriate, in which case the energy release rate is:

$$G_{III} = \frac{\tau_d^2(1+\nu^2)\pi a}{E} \quad (10)$$

where all the symbols are as defined above. These equations can also be written in terms of the openings (apertures) of the tension fractures and the displacements on the faults [Gudmundsson, 2011].

Energy input and power laws

Equations (6-10) show clearly that for a tension fracture (fig. 2) or a normal fault (fig. 3) to increase its length, that is, to propagate, potential energy must be provided and that this energy increases with increasing fracture surface area A and thus with increasing fracture length a. This conclusion can be used to explain, partly at least, the power-law size distributions of the fractures (figs. 4, 5). For a fracture to become relatively long, much energy is needed (fig. 8). To receive that energy, the fracture must be favourably orientated. The rose diagrams in figures 4 and 5 show that the fracture trend has a wide spread, but when normalised by length (weighted, fig. 4) the NE-trending fractures dominate. This follows because the NE-trending fractures are much longer than, say, NW-trending fractures in the datasets. The short NW-trending fracture thus almost disappear, whereas the weight of the long NE-trending fractures becomes much greater, when the data are normalised by length.

The results imply that only the NE-trending fractures become long and thus receive enough energy to propagate to great lengths. More specifically, within the rift zones only those fractures that trend perpendicular to the time-averaged direction of the local direction of spreading are likely to reach great lengths (and develop large surface areas). All rift-zone fractures that deviate in strike much from this direction, that is, fractures that are oblique, often at a large angle (for example, the NW-trending fractures), to the time-averaged direction of the local spreading direction, receive little potential energy, soon stop growing, and remain short.

In this view, the classes or bins in the power-low size distribution are a measure of energy levels. For a fracture to increase its length so as to move from one bin to the next to the right, energy input is needed (fig. 8) to overcome the surface energy (Eqs. 5, 6, 8). This means that, for a given energy input, only exceptionally favoured fractures as regards attitude and relation to the local stress field can reach relatively great lengths in a particular fracture network or population. It follows that as we move to the right on the 'energy scale' (fig. 8), there will gradually fewer fractures occupying the bins, resulting in a power-law length distribution of fractures.

These conclusions apply to other lineament networks – not only to natural but also to man-made lineaments. For example, figure 9 shows an analysis of the street networks of a typical medium-size European city, Dundee on the east coast of Scotland [Mohajeri and Gudmundsson, 2012]. The similarities with the fracture patterns are many: (1) most crustal fractures and streets are composed of segments; (2) both streets and fractures from parts of networks that evolve and expand through time; (3) the networks of street and fractures are confined to certain areas of certain shapes at any particular time, and their main trends follows roughly normal distributions (figs. 4, 5, 9); (4) the length ranges are similar: 0.1-7736 m for the fractures and 3-2249 m for the streets; (5) both streets and fractures show power-law length-size distributions that, on log-log plots, reveal subpopulations with different slopes or scaling exponents (figs. 4, 5, 9). These results are not unique for the streets of Dundee; street patterns of other cities are similar [Mohajeri, 2012] and, like fractures, show strong linear correlations between the entropy and the scaling exponents and length ranges.

Clearly, fractures and streets are not formed by the same mechanism. Both, however, relate to energy. The potential energy needed for a fracture to extend can be calculated from the equations discussed above, indicating that there is a given energy needed for a unit extension of a tectonic fracture of a given type. Similarly, there is a certain energy needed for a unit extension (construction) of a street of a given type [Commission, 2006]. Thus, an extra energy input is needed each time a fracture or a street is extended so as to move to a higher bin, that is, to a bin further to the

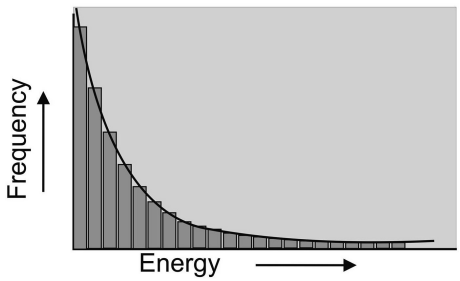

FIG. 8. – Schematic illustration of the energy needed for a fracture to increase its length so as to move from one bin to the next bin to the right. Moving to the right along the horizontal (energy) axis on the diagram, more and more energy is needed, so that fewer and fewer fractures have the energy input necessary to occupy the bins, hence the gradually decreasing height of the bins and the power-law size distribution.

right on the diagram in figure 8. This fact may indicate some general energy-related principles for many power-law size distributions and, in particular, those that relate to the size distributions of lineaments.

For any fracture network at a plate boundary (figs 1-3), the potential energy gradually increases during loading. When one or more large-scale fractures in the network form or start to propagate, strain energy is released (Eqs. 7, 8), the potential energy decreases and energy is dissipated and entropy produced. Plate-tectonic loading and input of potential energy shifts the fracture network (and the hosting volcanic system, fig. 1) again from a position of close-to equilibrium with the surroundings. The network (and its host rock) responses through fracture development (increasing material damage), that is, through forming new or propagating existing fractures at all scales, producing entropy, and approaching equilibrium again.

Entropy generally increases with increasing material damage [Kachanov, 1986]. Theoretical and experimental studies on entropy production during damage and fracture development, including applications to rock fractures [Majewski, 2000], confirm the general increase in entropy with damage [Yang *et al*., 2004; Hermann, 2007; Bao *et al*., 2010; Naderi *et al*., 2010; Qi *et al*., 2011]. For many materials, the cumulative entropy produced in relation to damage before large-scale failure is constant [Naderi *et al*., 2010; Qi *et al.,* 2011]. Also, some materials show a linear relation between entropy and applied stress [Qi *et al*., 2011], similar to that between strain and stress for many materials [Jaeger *et al*., 2007; Gudmundsson, 2011]. Considerations of the entropy evolution of rock-fracture networks may thus provide a basis for a better understanding of the energy input needed for fracture propagation and associated strain during large rifting evenings, earthquakes, and volcanic eruptions.

SUMMARY AND CONCLUSIONS

The results of a study of 565 tension fractures and normal faults associated with volcanic systems/fissure swarms at the divergent plate boundary in Iceland are presented. The fractures belong to four main networks/systems: two in Southwest Iceland and two in North Iceland. All the fractures dissect thick pahoehoe lava flow of Holocene age.

The fractures range in length from about 0.1 m to about 8 km and their length-size distributions follow power laws. Each fracture network can be divided into populations

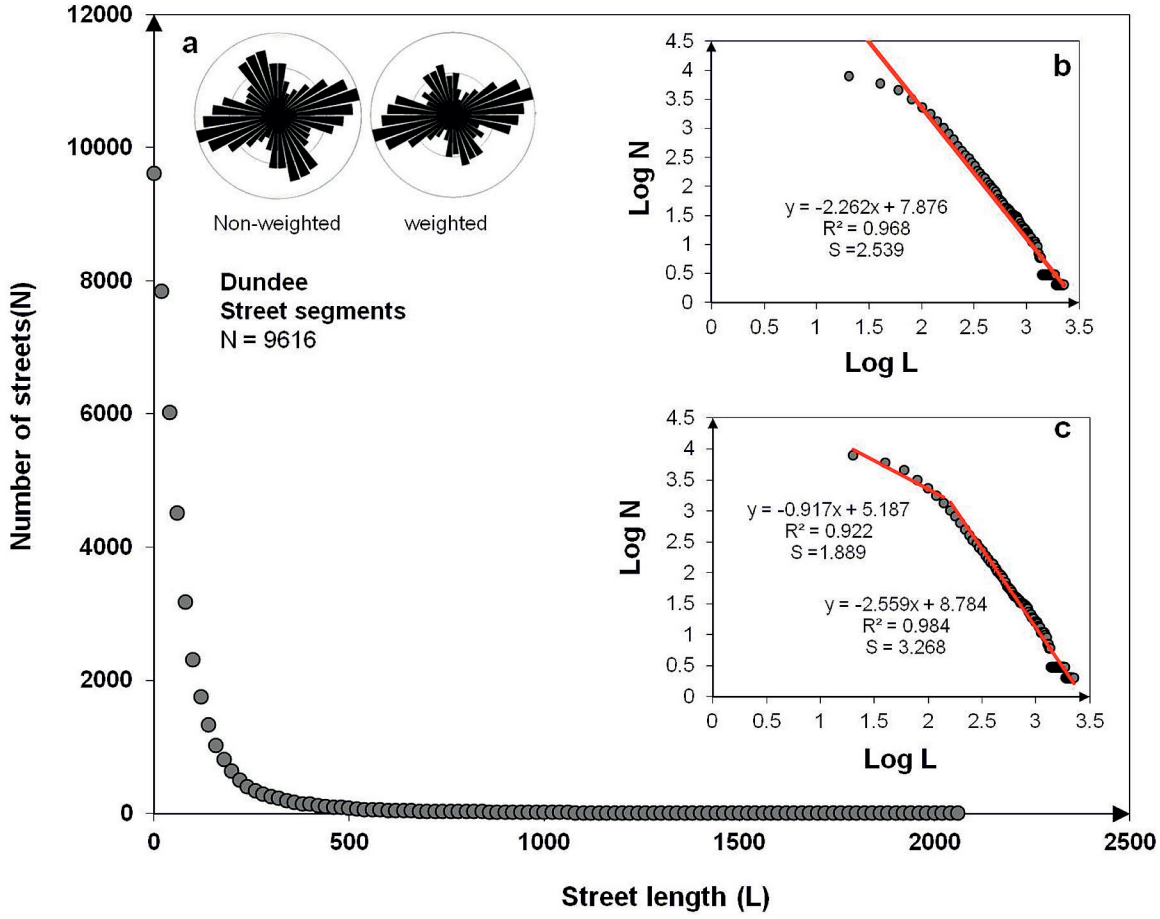

FIG. 9. – Power laws and breaks in scaling exponents for a total of 9616 streets in the city of Dundee, Scotland. (a) A cumulative power-law distribution for street lengths, and rose diagrams for the street trends (inset), non-weighted to the left and weighted to the right. The length is from 3 m to 2249 m, with an average length of 80 m. (b) Bi-logarithmic (log-log) plot of all the streets using a single power law. (c) Bi-logarithmic plot of all the streets using two (double) power laws. In figures (b, c) the break in the straight-line slopes indicates different street (sub)populations; the short streets have different functionality from the longer streets. The estimated coefficients of determination (R^2) and the entropies (S) are indicated. The scaling exponents of the street populations are indicated by the first terms on the right-hand side of the y-functions: 2.262 in (a) and 0.917 and 2.559 in (b).

based on abrupt changes in the scaling exponents of the power laws.

The scaling exponents of the fracture populations show strong linear correlations (r = 0.84) with their entropies, as calculated from the Gibbs entropy formula.

A relatively long power-law tail generally indicates a dispersed statistical distribution, that is, more energy spreading, and a comparatively high entropy. The length of the tail is proportional to the length range (the difference between the maximum and the minimum length) of fractures within each network/population. The present results show that the calculated entropies of the fracture populations vary positively as their length ranges and average lengths, thereby offering a physical basis for understanding the calculated entropies and their linear correlations with the scaling exponents of the populations.

The clear and strong linear correlation between the scaling exponents, entropies, length ranges, and average lengths of these fracture populations, together with the energy inputs needed for the fractures to grow, may be regarded as the first step in providing a fracture mechanics/thermodynamic theory for explaining the commonly observed power-law size distributions rock-fracture (and possibly other lineament) networks.

Acknowledgements. – We thank Sonja L. Philipp and Shigekazu Kusumoto for helpful review comments and Françoise Bergerat for the French translation of the title and the abstract.

References

Anderson T.L. (2005). – Fracture mechanics: Fundamentals and applications, 3rd ed. – Taylor & Francis, London, 621 p.

Andrew R.E.B. & Gumundsson A. (2007). – Distribution, structure, and formation of Holocene lava shields in Iceland. – *J. Volcanol. Geotherm. Res*., **168**, 137-154.

Atkins A.G. & Mai Y.W. (1985). – Elastic and plastic fracture. – Ellis Horwood, Chichester, 1198 p.

Baierlein R. (1971). – Atoms and information theory: An introduction to statistical mechanics. – W.H. Freeman, San Francisco, 486 p.

Baierlein R. (1999). – Thermal physics. – Cambridge University Press, Cambridge, 460 p.

Bao T.F., Peng Y., Cong P.J. & Wang J.L. (2010). – Analysis of crack propagation in concrete structures with structural information entropy. – *Sci. China Technol. Sci.,* **53**, 1943-1948.

Barabasi A.L. & Albert R. (1999). – Emergence of scaling in random networks. – *Science*, **286**, 509-512.

Ben-Naim A. (2008). – Farewell to entropy: Statistical thermodynamics based on information. – World Scientific, London, 412 p.

Berkowitz B., Bour O., Davy P. & Odling N. (2000). – Scaling of fracture connectivity in geological formations. – *Geophys. Res. Lett.,* **27**, 2061-2064.

Blundell S.J. & Blundell K.M. (2010). – Concepts in thermal physics, 2nd ed. – Oxford University Press, Oxford, 493 p.

Bonnet E., Bour O., Odling N.E., Davy P., Main I., Cowie P. & Berkowitz B. (2001). – Scaling of fracture systems in geological media. – *Rev. Geophys.*, **39**, 347-383.

Bour O. & Davy P. (1998). – On the connectivity of three-dimensional fault networks. – *Water Resour. Res*., **34**, 2611-2622.

Commission (2006). – Integration of the measurement of energy usage into road design. – Brussel, Commission of the European Communities Directorate-General for Energy and Transport. – Final report, Project number 4.1031/Z/02-09/2002.

Griffith A.A. (1920). – The phenomena of rupture and flow in solids. – *Phil. Trans. R. Soc. Lond.*, **A221**, 163-198.

Gudmundsson A. (1987a). – Geometry, formation and development of tectonic fractures on the Reykjanes peninsula, southwest Iceland. – *Tectonophysics*, **139**, 295-308.

Gudmundsson A. (1987b). – Tectonics of the Thingvellir fissures, SW Iceland. – *J. Struct. Geol.,* **9**, 61-69.

Gudmundsson A. (1992). – Formation and growth of normal faults at the divergent plate boundary in Iceland. – *Terra Nova*, **4**, 464-471.

Gudmundsson A. (2011). – Rock fractures in geological processes. – Cambridge University Press, Cambridge, 592 p.

Hatton C.G., Main I.G. & Meredith P.G. (1994). – Non-universal scaling of fracture length and opening displacement. – *Nature*, **367**, 160-162.

Hermann G. (2007). – A thermodynamic theory of damage in elastic inorganic and organic solids. – *Arch. Appl. Mech.,* **77**, 123-133.

Jaeger J.C., Cook N.G.W. & Zimmerman R.W. (2007). – Fundamentals of rock mechanics, 4th ed. – Blackwell, Oxford, 488 p.

Jaynes E.T. (1957a). – Information theory and statistical mechanics. – *Phys. Rev.,* **106**, 620-630.

Jaynes E.T. (1957b). – Information theory and statistical mechanics. II. – *Phys. Rev.*, **108**, 171-190.

Kachanov L.M. (1986). – Introduction to continuum damage mechanics. – Martinus Nijhoff, Dordrecht, 148 p.

Laurendau N.M. (2005). – Statistical thermodynamics. Fundamentals and applications. – Cambridge University Press, Cambridge, 466 p.

Leff H.S. (1999). – What if entropy were dimensionless? – *Am. J. Phys*., **67**, 1114-1122.

Majewski E. (2000). – Thermodynamics of fault slip. *In*: R. TEISSEYRE & E. MAJEWSKI, Eds., Earthquake thermodynamics and phase transformations in the Earth's interior. – Academic Press, London, 323-328.

Mays D.C., Faybishenko B.A. & Finsterle S. (2002). – Information entropy to measure temporal and spatial complexity of unsaturated flow in heterogeneous media. – *Wat. Resourc. Res.,* **38**, 12, 1313, doi: 10.1029/2001WR001185.

Mishnaevsky L. (1998). – Damage and fracture in heterogeneous materials. – Balkema, Rotterdam, 200 p.

Mishnaevsky L. (2007). – Computational mesomechanics of composites. – New York, Wiley, 294 p.

Mohajeri N. (2012). – Effects of landscape constraints on street patterns in cities: Examples from Khorramabad, Iran. – *Appl. Geogr.*, **34**, 10-20.

Mohajeri N. & Gudmundsson A. (2012). – Entropies and scaling exponents of street and fracture networks. – *Entropy*, **14**, 800-833.

Naderi M., Amiri M. & Khosari M.M. (2010). – On the thermodynamic entropy of fatigue fracture. – *Proc. R. Soc. Lond*., **A466**, 423-438.

Newman M.E.J. (2005). – Power laws, Pareto distributions and Zipf's law. – *Contemp. Phys.,* **46**, 323-351.

Nieto-Samaniego A.F., Alaniz-Alvarez S.A., Tolson G., Oleschko K., Korvin G., Xu S.S. & Perez-Venzor J.A. (2005). – Spatial distribution, scaling and self-similar behaviour of fracture arrays in the Los Planes fault, Baja California Sur, Mexico. – *Pure Appl. Geophys.,* **162**, 805-826.

Qi G., Wayne S.F. & Fan M. (2011). – Measurements of a multicomponent variate in assessing evolving damage states in a polymeric material.I – *EEE Trans. Instr. Measurem.*, **60**, 206-213.

Rice J.R. (1978). – Thermodynamics of the quasi-static growth of Griffith cracks. – *J. Mech. Phys. Solids*, **26**, 61-78.

Rossi M. (1996). – Morphology and mechanism of eruption of postglacial lava shields in Iceland. – *Bull. Volcanol*., **57**, 530-540.

Sethna J.P. (2006). – Statistical mechanics: entropy, order parameters, and complexity. – Oxford University Press, Oxford, 376 p.

SINGH V.P. (1997). – Effect of class-interval size on entropy. – *Stochastic Hydol. Hydraulics*, **11**, 423-431.

STEVENS R.N. & GUIU F. (1991). – Energy balance concepts in the physics of fracture. – *Proc. R. Soc. Lond.,* **A435**, 169-184.

THORDARSON T. & HOSKULDSSON A. (2008). – Postglacial volcanism in Iceland. – *Jokull*, **58**, 197-228.

TOYABE S., SAGAWA T., UEDA M., MUNEYUKI E. & SANO M. (2010). – Experimental demonstration of information-to-energy conversion and validation of the generalized Jarzynski equality. – *Nature Phys*., **6**, 988-992.

TURCOTTE D. (1997). – Fractals and chaos in geology and geophysics, 2nd ed. – Cambridge University Press, Cambridge, 416p.

VOLKENSTEIN M.V. (2009). – Entropy and information. – Birkhauser, Berlin, 209 p.

WEI R.P. (2010). – Fracture mechanics. – Cambridge University Press, Cambridge, 230 p.

XIE H. (1993). – Fractals in rock mechanics. – Balkema, Rotterdam, 464 p.

YANG Q., THAM L.G. & SWOBODA G. (2004). – Relationship between refined Griffith criterion and the power laws for cracking. – *Mech. Res. Comm*., **31**, 429-434.